

Supplementary Table 1. Characteristics of the organoids

ID	Gender	Type	Grade	T (cm)	LN pos	LN	ER	PR	HER2	KI67	LVI
1	Female	IDC	III	2.6	0	28	-	-	-	80%	+
2	Female	IDC	III	5.5	25	27	-	-	-	70%	+
3	Female	IDC	III	2.5	0	4	-	-	-	35%	-

IDC: invasive ductal carcinoma; T: tumor size; LN pos: the number of positive lymph nodes; LN: the number of total lymph nodes measured; ER: estrogen receptor; PR: progestogen receptor; HER2: human epidermal growth factor receptor 2; LVI: lymphovascular invasion

Supplementary Table 2. Clinicopathological features of the mini-PDXs

Sample ID	Gender	TNM	Grade	Histopathologic type	ER	PR	HER2
543	Female	T2N0M0	II	IDC	-	-	-
552	Female	T2N0M0	II	IDC	-	-	-
553	Female	T2N0M0	III	IDC	-	-	-
554	Female	T1N0M0	III	IDC	-	-	-
573	Female	T2N1M0	III	IDC	-	-	-
578	Female	T1N0M0	II	IDC	-	-	-
584	Female	T1N1M0	III	IDC	-	-	-

T: tumor size; N: lymph node; M: metastasis; IDC: invasive ductal carcinoma; ER: estrogen receptor; PR: progestogen receptor; HER2: human epidermal growth factor receptor 2.

Supplementary Table 3. Multivariate cox regression analysis of RFS in 138 primary TNBC

	Univariate Cox		Multivariate Cox	
	HR (95% CI)	P value	HR (95% CI)	P value
ENSA IHC score	2.4 (1.17-4.95)	0.02	2.27 (1.06-4.86)	0.04
Age	0.41 (0.20-0.84)	0.01	0.51 (0.24-1.09)	0.08
Tumor size	0.95 (0.38-2.36)	0.9	0.77 (0.31-1.92)	0.57
Lymph node	2.16 (1.04-4.49)	0.04	2.28 (1.06-4.91)	0.03
N1-3 vs. N0				

RFS: relapse-free survival; TNBC: triple-negative breast cancer; HR: hazard ratio; CI: confidence intervals; IHC: immunohistochemistry

Supplementary Table 4. Multivariate cox regression analysis of OS in 138 primary TNBC

	Univariate Cox		Multivariate Cox	
	HR (95% CI)	P value	HR (95% CI)	P value
ENSA IHC score	4.1 (1.16-14.56)	0.03	1.36 (0.97-1.91)	0.07
Age	0.24 ≥50y vs. <50y (0.06-0.92)	0.04	0.34 (0.08-1.41)	0.13
Tumor size	2.42 ≥2cm vs. <2cm (0.30-19.33)	0.41	1.59 (0.19-12.96)	0.66
Lymph node	3.25 N1-3 vs. N0 (0.84-12.58)	0.09	2.78 (0.69-11.24)	0.15

OS: overall survival; TNBC: triple-negative breast cancer; HR: hazard ratio; CI: confidence intervals; IHC: immunohistochemistry

Supplementary Table 5. A list of primers for RT-qPCR

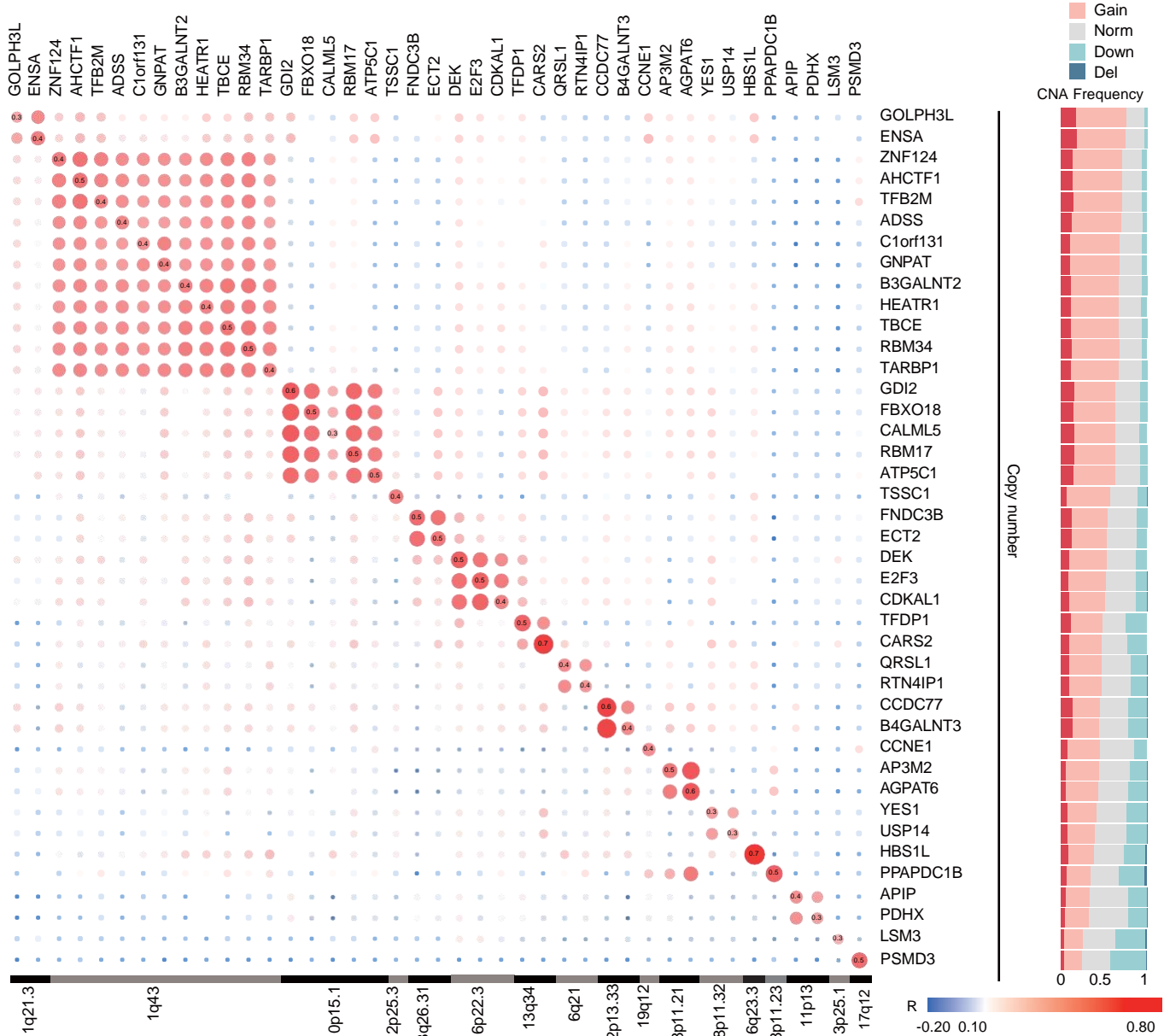
ENSA-Forward	AGGCAAAGCTAAAGGCCAAT
ENSA-Reverse	GCCATGTTGTAGTCTCCTGAGT
FDPS-Forward	TGTGACCGGCAAAATTGGC
FDPS-Reverse	GCCCGTTGCAGACACTGAA
DHCR7-Forward	GCTGCAAAATCGCAACCCAA
DHCR7-Reverse	GCTCGCCAGTGAAAACCAGT
FDFT1-Forward	CCACCCGAAGAGTTCTACAA
FDFT1-Reverse	TGCGACTGGTCTGATTGAGATA
ACAT2-Forward	GCGGACCATCATAGGTTCCCTT
ACAT2-Reverse	ACTGGCTTGTCTAACAGGATTCT
HMGCR-Forward	TGATTGACCTTCCAGAGCAAG
HMGCR-Reverse	CTAAAATTGCCATTCCACGAGC
EBP-Forward	CTCAGCACCTAAGACTGGACA
EBP-Reverse	ACGACTAAGACCCCTGTGACA
MVD-Forward	CTCCCTGAGCGTCACTCTG
MVD -Reverse	GGTCCTCGGTGAAGTCCTTG
MVK -Forward	CATGGCAAGGTAGCACTGG
MVK -Reverse	GATACCAATGTTGGTAAGCTGA
LSS-Forward	GCACGGACGGGTGATTATGG
LSS-Reverse	TCTCTTCTCTGTATCCGGCTG
SREBF2-Forward	AACGGTCATTCACCCAGGTC
SREBF2-Reverse	GGCTGAAGAATAGGAGTTGCC
GAPDH-Forward	GGAGCGAGATCCCTCCAAAAT
GAPDH-Reverse	GGCTGTTGTCATACTTCTCATGG
HMGCS1-Forward	GATGTGGATTGTTGCCCTT
HMGCS1-Reverse	ATTGTCTCTGTTCCAACCTCCAG

RT-qPCR: real-time quantitative reverse transcription.

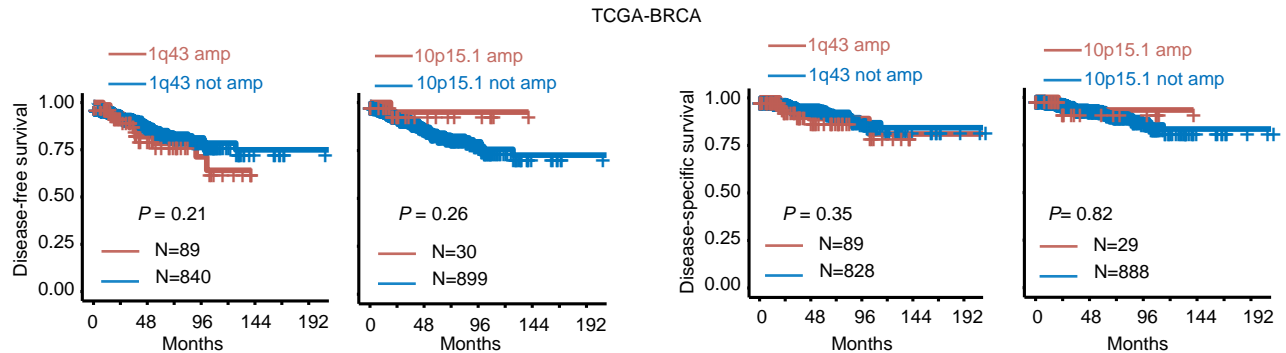
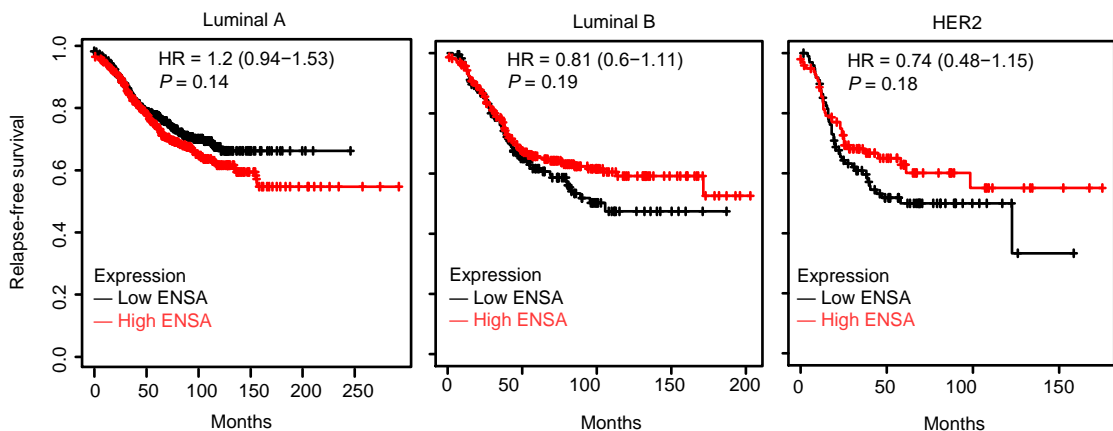
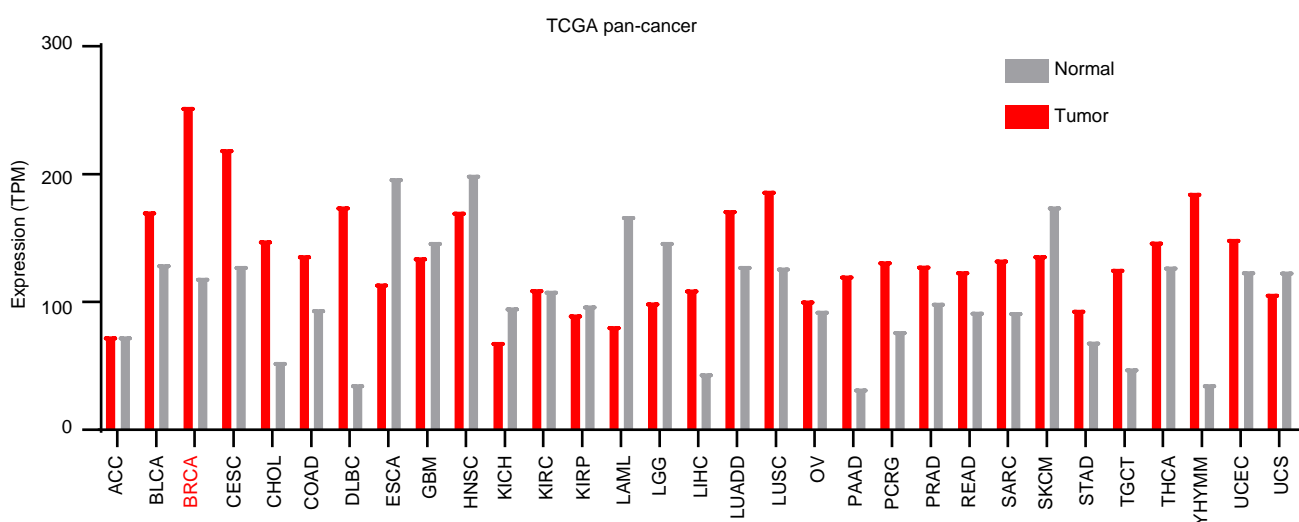
Supplementary Table 6. Detailed antibody usage

Name	Company	Application	Dilution	Cat #
ENSA	Abcam	Immunoblot	1:10000	ab180513
ENSA	Proteintech	IHC	1:100	14518-1-AP
MVK	Affinity	Immunoblot	1:1000	DF3238
FDPS	Proteintech	Immunoblot; IHC	WB: 1:3000; IHC: 1:200	16129-1-AP
ACAT2	Abcam	Immunoblot	1:3000	ab131215
SREBP2	Abcam	Immunoblot; IHC	WB: 1:1000; IHC: 1:100	ab30682
SREBP2	Proteintech	IHC	1:200	28212-1-AP
LSS	Abcam	Immunoblot	1:3000	ab140124
FDFT1	Abcam	Immunoblot	1:3000	ab195046
HMGCR	Abcam	Immunoblot	1:3000	ab174830
HMGCS1	Proteintech	Immunoblot	1:1000	17643-1-AP
FLAG	Sigma-Aldrich	Immunoblot	1:1000	F1804
p-STAT3 (Tyr705)	Cell Signaling	Immunoblot; IHC	1:2000	9145
p-STAT3 (Ser 727)	Cell Signaling	Immunoblot	1:1000	9134
STAT3	Cell Signaling	Immunoblot; ChIP	WB: 1:1000; ChIP: 4µg	9139
PP2AC	Cell Signaling	Immunoblot	1:2000	2038
GAPDH	Proteintech	Immunoblot	1:10000	60004-1-Ig
alpha tubulin	Proteintech	Immunoblot	1:3000	11224-1-AP
mouse IgG2a isotype	Cell Signaling	ChIP	4ug	61656
HRP-linked anti- mouse antibodies	Proteintech	Immunoblot	1:5000	SA00001-1
HRP-linked anti- rabbit antibodies	Proteintech	Immunoblot	1:5000	SA00001-2

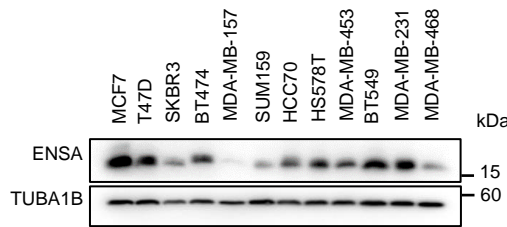
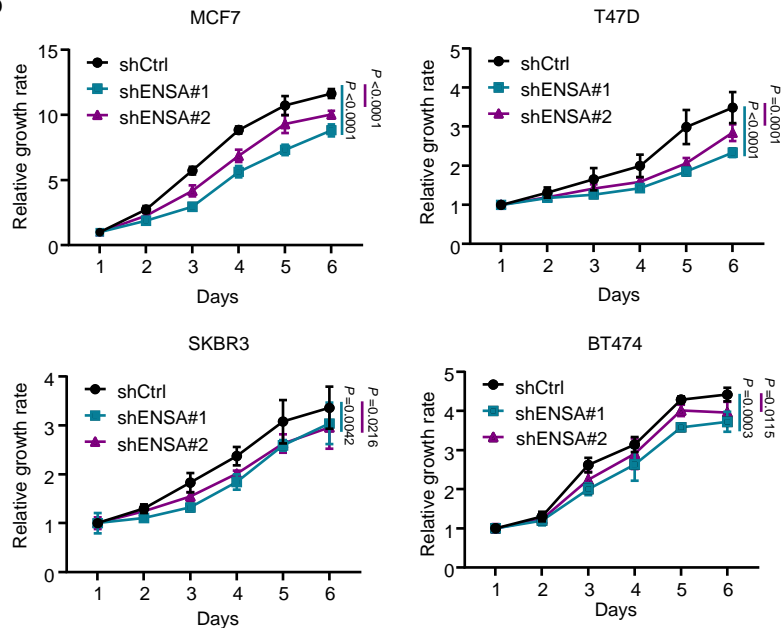
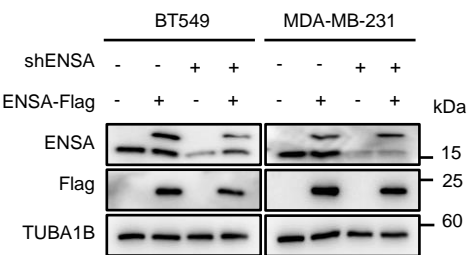
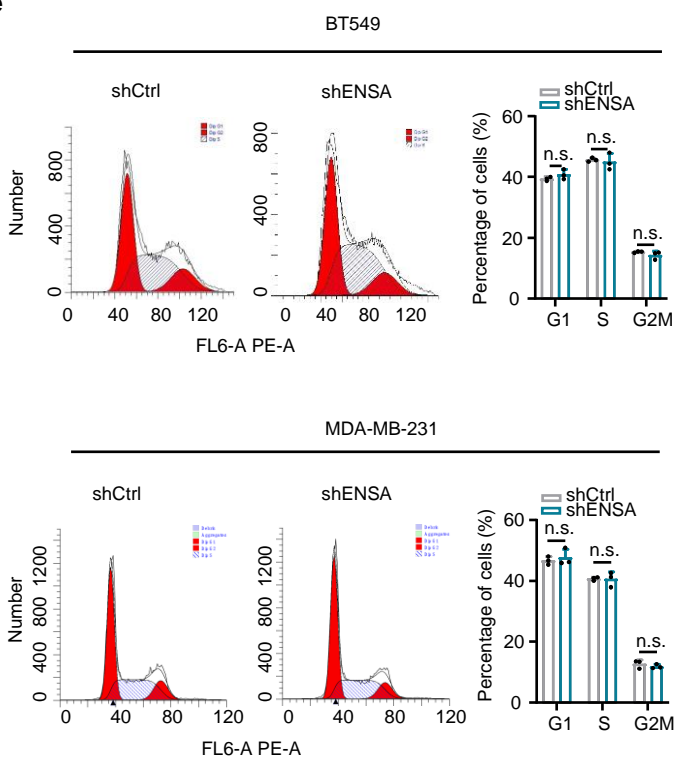
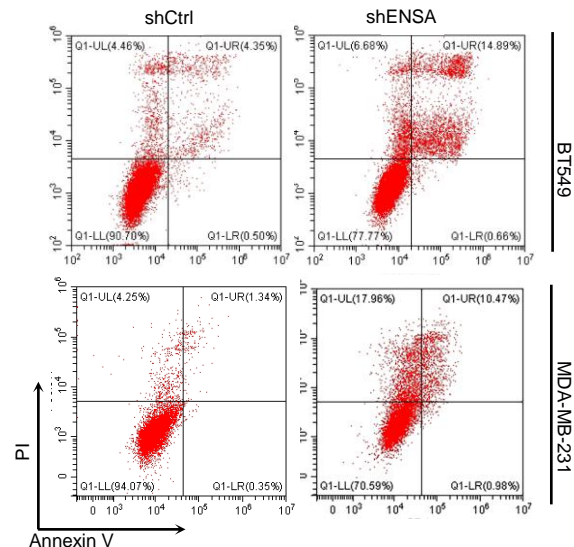
Gene expression



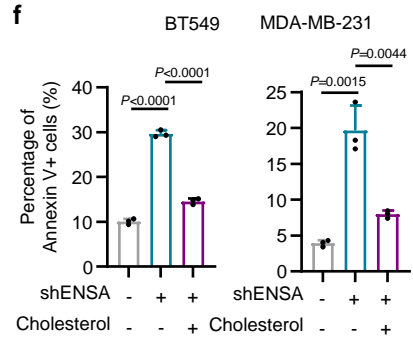
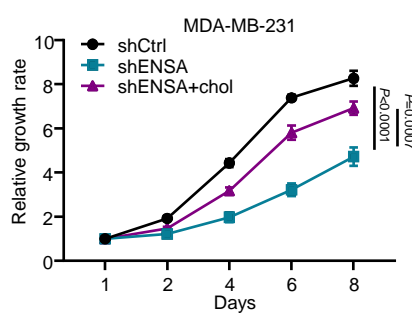
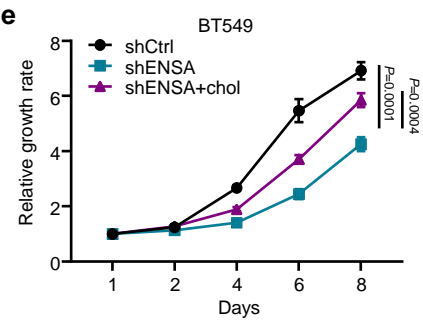
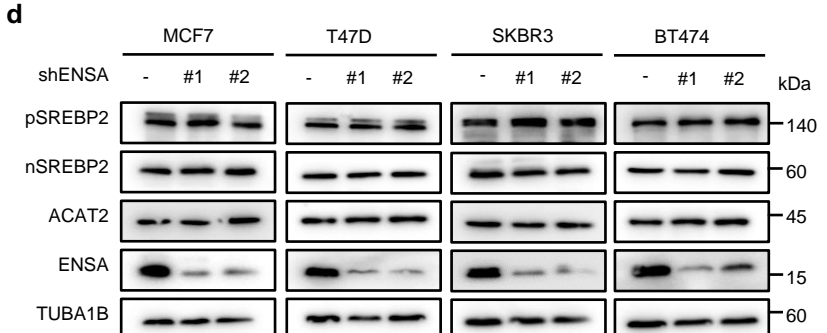
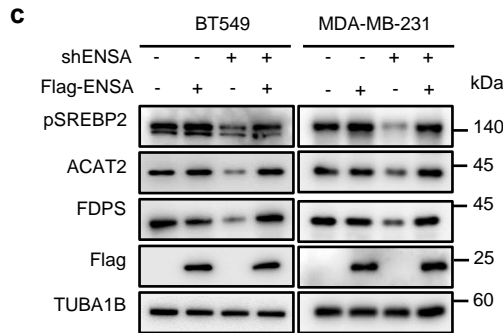
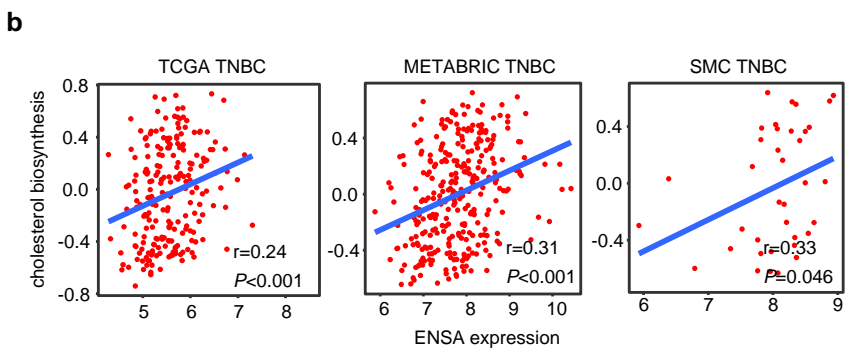
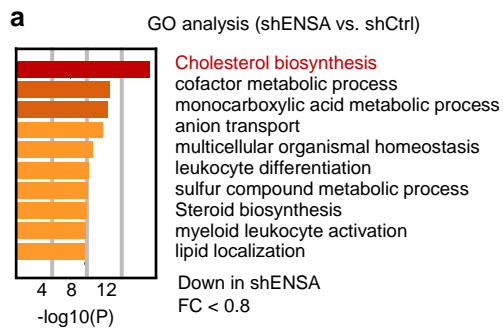
Supplementary Fig. 1 The correlation between the expression and copy number of 41 candidates in 302 TNBC patients according to both RNA-seq data and copy number data. Genes were ranked by amplification and gain frequency. Correlation coefficients were calculated using the Pearson test. Amp, amplification; Norm, normal; Del, deletion.

a**b****c**

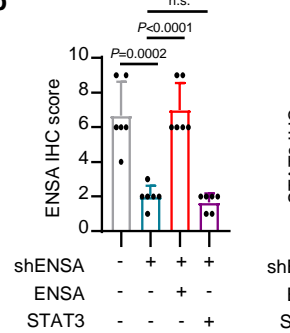
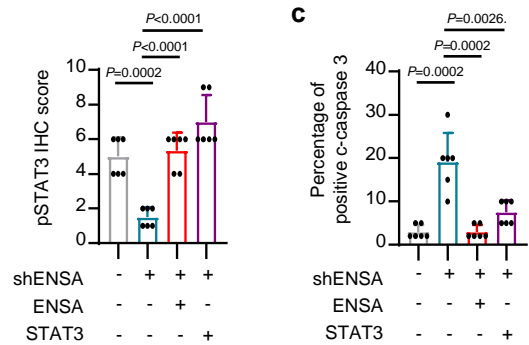
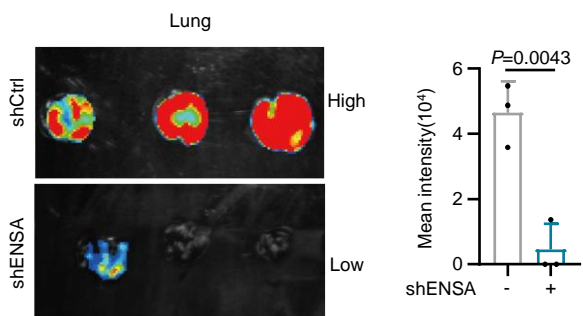
Supplementary Fig. 2 ENSA transcriptome profile in breast cancer. (a) Kaplan-Meier survival analysis of 1q43 and 10p15.1 copy number alteration in TCGA breast cancer patients. Log-rank test. (b) Kaplan-Meier plots of ENSA in the luminal A, luminal B and HER2 subtypes (<https://kmplot.com/analysis/>). Log-rank test. (c) ENSA mRNA levels in different cancers from the TCGA cohort. TCGA, The Cancer Genome Atlas; BRCA, breast cancer; amp, amplification. TPM, transcripts per million.

a**b****c****e****d**

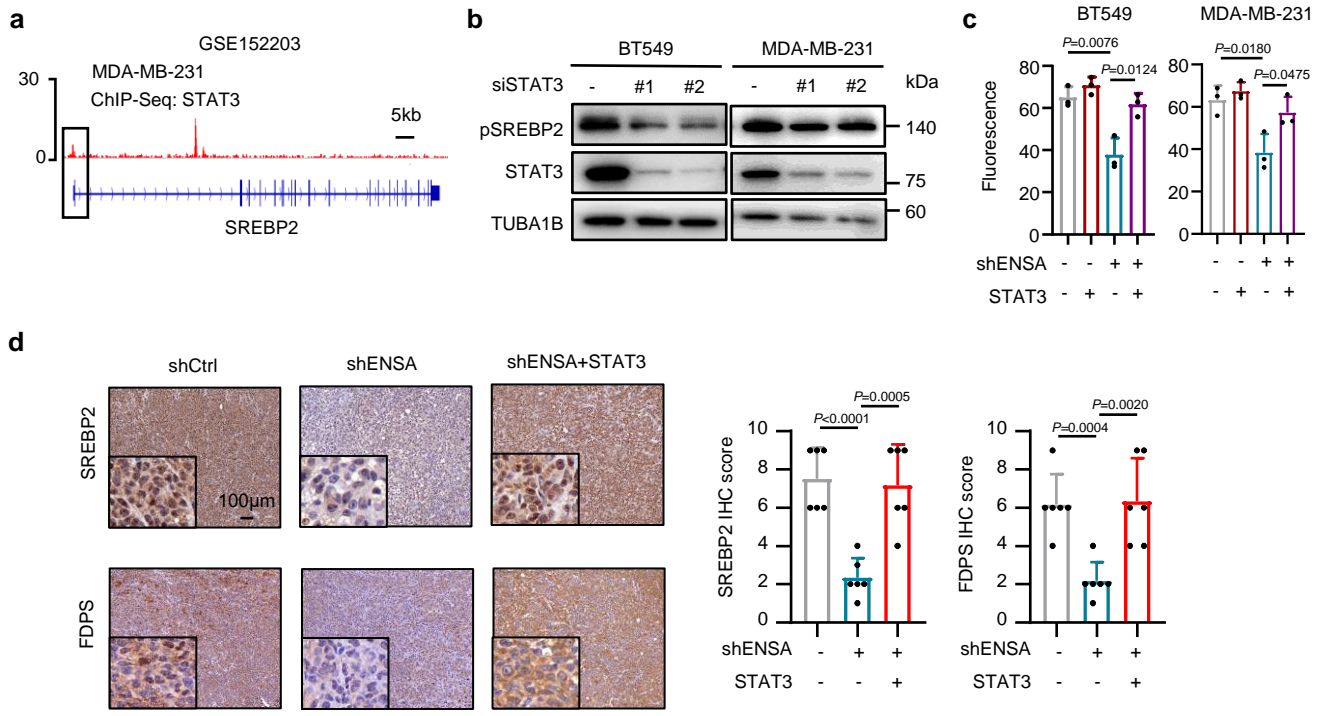
Supplementary Fig. 3 ENSA promotes the survival of TNBC cells. **(a)** The protein expression of ENSA across multiple breast cancer cell lines. **(b)** In vitro growth curves of MCF7, T47D, SKBR3, and BT474 cells expressing control or ENSA shRNA. n=6. Data are presented as mean ± SD. Two-tailed two-way ANOVA tests. **(c)** Empty vector or flag-tagged ENSA overexpression vector was transfected into BT549 and MDA-MB-231 cells expressing control or ENSA shRNA. **(d)** Representative images of cell apoptosis in BT549 and MDA-MB-231 cells expressing control or ENSA shRNA. **(e)** Cell cycle distribution measured in BT549 and MDA-MB-231 cells expressing control or ENSA shRNA. Representative images and the percentage of cells in the G1/S/G2M phase are shown. n=3. Data are presented as mean ± SD. Two-tailed unpaired Student's t tests. Source data are provided as a Source Data file. n.s., not significant.



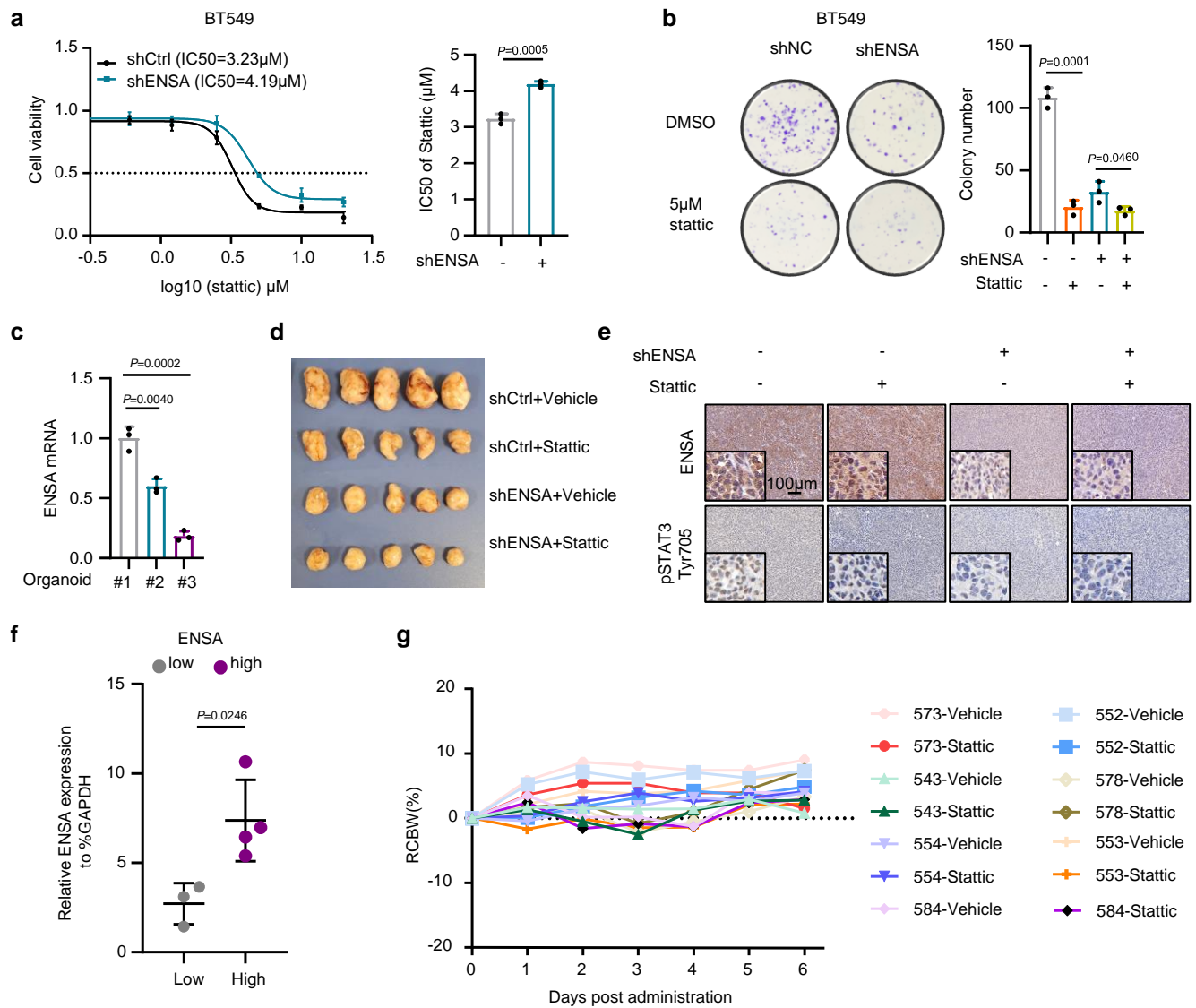
Supplementary Fig. 4 ENSA impacts cholesterol biosynthesis in TNBC. **(a)** GO analysis of downregulated genes after ENSA knockdown in MDA-MB-231 cells. Top 10 pathways according to $-\log_{10}(P$ value) are shown. **(b)** Scatter plot showing the correlation of ENSA expression with the cholesterol biosynthesis pathway score in TCGA, METABRIC and SMC TNBC data identified by ‘gsva’ method. Correlation coefficients were calculated using the *Pearson* test. Two-tailed P -values were given. **(c)** Western blotting images showing proteins involved in the cholesterol biosynthesis pathway in BT549 and MDA-MB-231 cells \pm ENSA knockdown and \pm ENSA overexpression. n=3 independent experiments. **(d)** Western blotting images showing proteins involved in the cholesterol biosynthesis pathway after ENSA knockdown in non-TNBC breast cancer cells. n=3 independent experiments. **(e)** In vitro growth curves of BT549 and MDA-MB-231 cells expressing control or ENSA shRNA after treatment with 2.5 $\mu\text{g}/\text{ml}$ exogenous cholesterol. n=3. Data are presented as mean \pm SD. Two-tailed two-way ANOVA tests. **(f)** Cell apoptosis measured in BT549 and MDA-MB-231 cells expressing control or ENSA shRNA after treatment with 2.5 $\mu\text{g}/\text{ml}$ exogenous cholesterol. n=3. Data are presented as mean \pm SD. Two-tailed unpaired Student's t tests. Source data are provided as a Source Data file. GO, Gene Ontology; FC, fold change; TCGA, The Cancer Genome Atlas; METABRIC, Molecular Taxonomy of Breast Cancer International Consortium; SMC, a Korean breast cancer cohort; chol, cholesterol.

a**b****c****d**

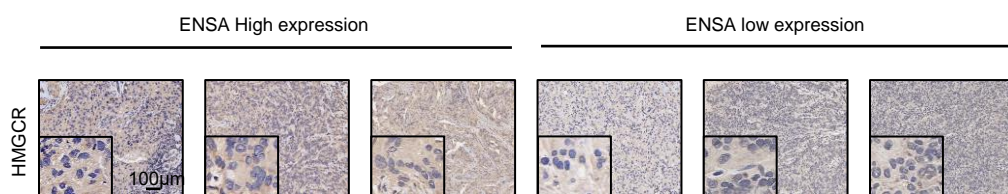
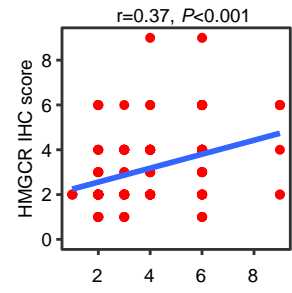
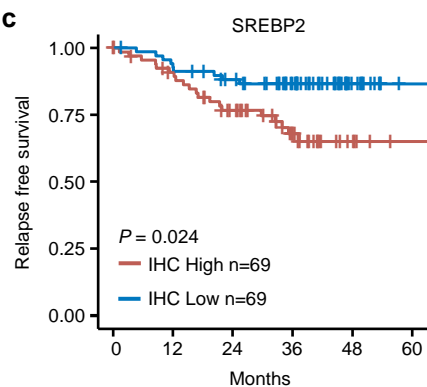
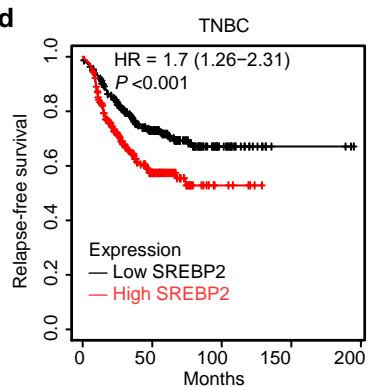
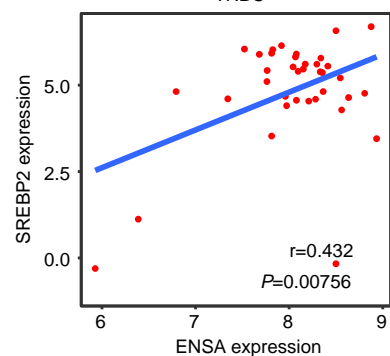
Supplementary Fig. 5 ENSA/STAT3 promotes TNBC progression in vivo. (a) Representative images of tumors generated by injecting MDA-MB-231 cells expressing control or ENSA shRNA and rescued by ENSA or STAT3 overexpression. (b) Immunohistochemical scores of ENSA and pSTAT3-Tyr705 in mouse mammary fat pad xenograft models generated by injecting MDA-MB-231 cells expressing control or ENSA shRNA and rescued by ENSA or STAT3 overexpression. n=6. Data are presented as mean \pm SD. Two-tailed unpaired Student's t tests. (c) Percentage of cleaved caspase 3-positive cells in mouse mammary fat pad xenograft models. n=6. Data are presented as mean \pm SD. Two-tailed unpaired Student's t tests. (d) The bioluminescence intensities of lung metastasis of MDA-MB-231 cells expressing control or ENSA shRNA. n=3. Data are presented as mean \pm SD. Two-tailed unpaired Student's t tests. Source data are provided as a Source Data file. c-caspase 3, cleaved caspase 3. n.s., not significant.



Supplementary Fig. 6 ENSA mediates the transcriptional activation of SREBP2 via PP2A-STAT3. **(a)** STAT3 ChIP-seq signal in MDA-MB-231 cells at the genomic location adjacent to the SREBP2 promoter from GSE152203. **(b)** Western blotting images showing SREBP2 expression in BT549 and MDA-MB-231 cells expressing control or STAT3 siRNA. **(c)** Fluorescence quantification of Filipin staining. n=3. Data are presented as mean \pm SD. Two-tailed unpaired Student's t tests. **(d)** Immunohistochemical images and scores of SREBP2 and FDPS in mouse mammary fat pad xenograft models generated by injecting MDA-MB-231 cells expressing control or ENSA shRNA and rescued by STAT3 overexpression. n=6. Data are presented as mean \pm SD. Two-tailed unpaired Student's t tests. Source data are provided as a Source Data file. IHC, immunohistochemistry.

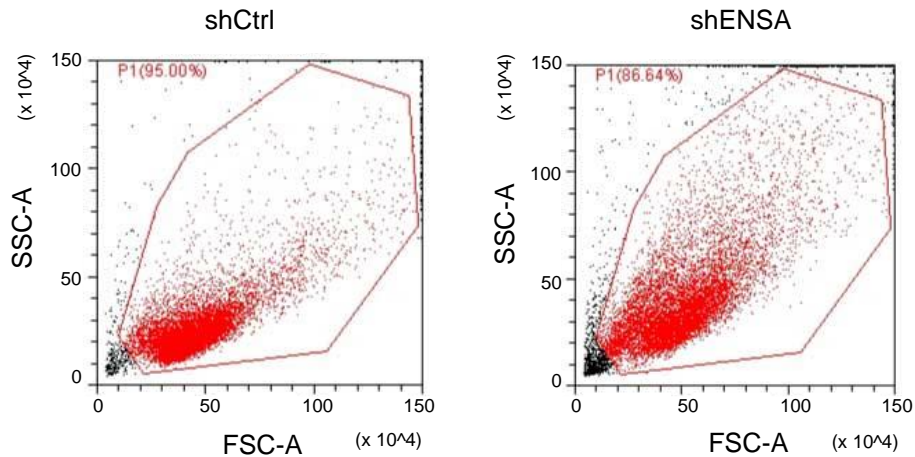


Supplementary Fig. 7 ENSA determines sensitivity to Stattic in TNBC. **(a)** Dose-response curves and half maximal inhibition concentration values of stattic in BT549 cells expressing control or ENSA shRNA. Dose-response curves: n=6; Data are presented as mean \pm SD. Bar plot: n=3 independent experiments; Data are presented as mean \pm SD; Two-tailed unpaired Student's t test. **(b)** Clonogenic survival assays of BT549 cells expressing control or ENSA shRNA and treated with 5 μ M stattic. n=3. Data are presented as mean \pm SD. Two-tailed unpaired Student's t test. **(c)** qRT-PCR detecting relative ENSA mRNA expression in TNBC organoids. n=3. Data are presented as mean \pm SD. Two-tailed unpaired Student's t test. **(d)** Representative images of tumors generated by injecting MDA-MB-231 cells expressing control or ENSA shRNA and treating with vehicle or Stattic (10 mg/kg). **(e)** Immunohistochemical images of ENSA and pSTAT3-Tyr705 in mouse mammary fat pad xenograft models. n=3 independent experiments. **(f)** qRT-PCR detecting relative ENSA mRNA expression in TNBC mini-PDX models. n=3 in low-ENSA group and n=4 in high-ENSA group. Data are presented as mean \pm SD. Two-tailed unpaired Student's t test. **(g)** Relative body weight changes of mini-PDX-bearing mice. Source data are provided as a Source Data file. RCBW, relative change of body weight.

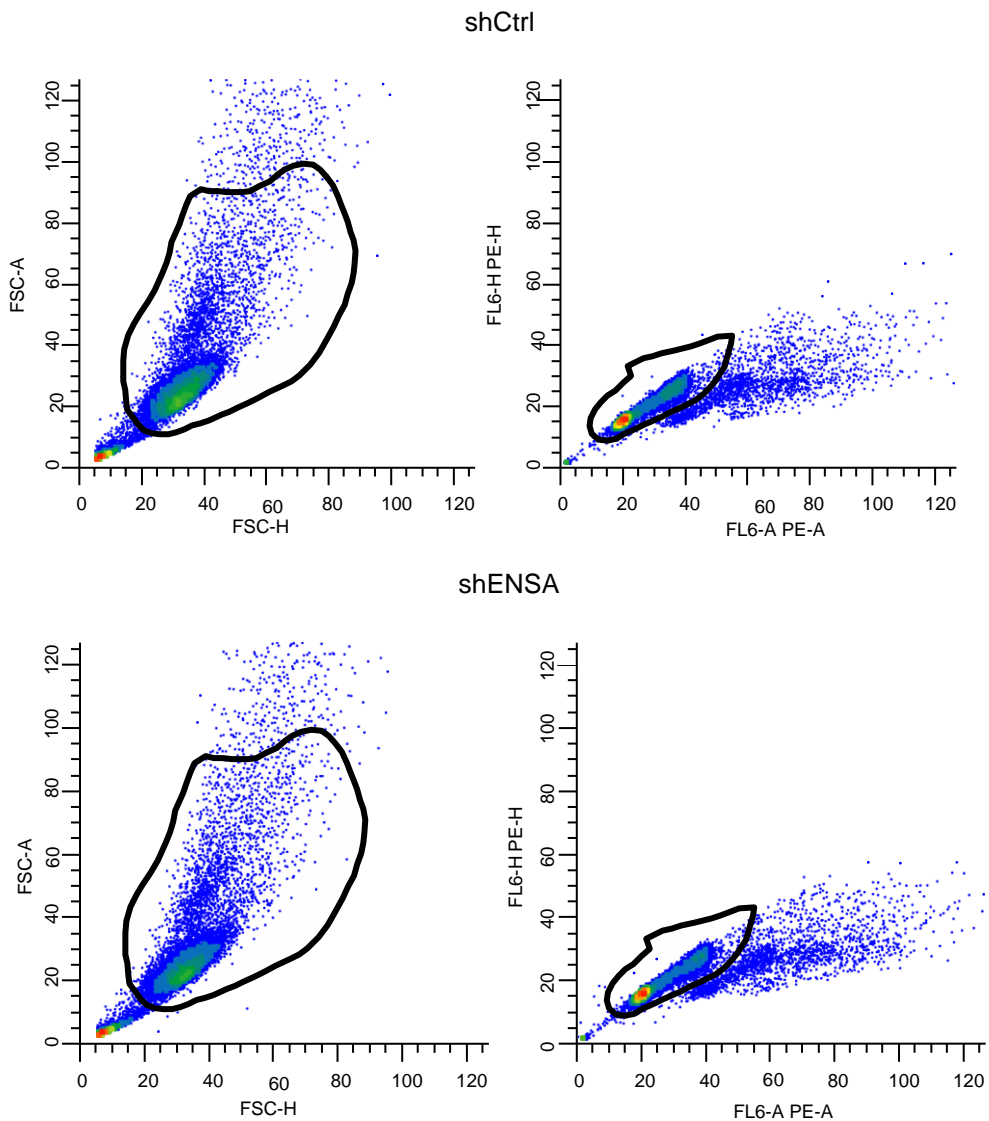
a**b****c****d****e**

Supplementary Fig. 8 Correlation of ENSA and downstream pathways. **(a)** Representative IHC images of HMGCR staining in 138 TNBC specimens. Representative images are shown. Scale bars, 100 μ m. **(b)** Correlation analysis of ENSA and HMGCR expression levels in 138 TNBC tissues. Correlation coefficients were calculated using the *Spearman* test. Two-tailed P -values were given. **(c)** Kaplan-Meier analysis of SREBP2 IHC expression on the relapse-free survival of 138 TNBC patients. Log-rank test. **(d)** Kaplan-Meier plots of SREBP2 in TNBC (<https://kmplot.com/analysis/>). Log-rank test. **(e)** Correlation analysis of ENSA and SREBP2 expression in an Asian breast cancer cohort (SMC cohort, Korea). n=37 TNBC patients. Correlation coefficients were calculated using the *Pearson* test. Two-tailed P -values were given. IHC, immunohistochemistry.

Supplementary Fig. 9 Representative image of FACS sequential gating/sorting strategies of MDA-MB-231 depicted in Supplementary Fig. 3d.



Supplementary Fig. 10 Representative image of FACS sequential gating/sorting strategies of MDA-MB-231 depicted in Supplementary Fig. 3e.



Supplementary Fig. 11 Representative image of FACS sequential gating/sorting strategies of MDA-MB-231 depicted in Supplementary Fig. 4f.

